

Few-Shot Continual Learning for Conditional Generative Adversarial Networks

Cat P. Le, Juncheng Dong, Ahmed Aloui, Vahid Tarokh

Department of Electrical and Computer Engineering, Duke University
 {cat.le, juncheng.dong, ahmed.aloui, vahid.tarokh}@duke.edu

Abstract

In few-shot continual learning for generative models, a target mode must be learned with limited samples without adversely affecting the previously learned modes. In this paper, we propose a new continual learning approach for conditional generative adversarial networks (cGAN) based on a new mode-affinity measure for generative modeling. Our measure is entirely based on the cGAN’s discriminator and can identify the existing modes that are most similar to the target. Subsequently, we expand the continual learning model by including the target mode using a weighted label derived from those of the closest modes. To prevent catastrophic forgetting, we first generate labeled data samples using the cGAN’s generator, and then train the cGAN model for the target mode while memory replaying with the generated data. Our experimental results demonstrate the efficacy of our approach in improving the generation performance over the baselines and the state-of-the-art approaches for various standard datasets while utilizing fewer training samples.

1 Introduction

Artificial intelligence (AI) for generative tasks has made significant progress in recent years, and we have seen remarkable applications, such as ChatGPT [1], DALL-E [2], and deepfake [3]. However, most of these methods [4, 5, 6, 7, 8] lack the ability to learn continuously, which remains a challenging problem in developing AI models that can match human’s continuous learning capabilities. This challenge is particularly difficult when the target data is limited or scarce, as in few-shot continual learning for image generation [5, 6, 8]. In this scenario, the goal is to learn to generate new images using an extensive model that is trained on all previous tasks. Most continual learning methods focus on preventing the models from forgetting the existing tasks, but many learning restrictions are often enforced on learning new tasks, leading to poor performance. To efficiently learn the new task, relevant knowledge can be identified and utilized. To this end, various knowledge transfer approaches have been introduced, resulting in significant breakthroughs in many applications, including natural language processing [9, 10, 11, 12, 13], and image classification [14, 15, 16, 17, 18, 19]. These techniques enable models to leverage past experiences, such as trained models, and hyper-parameters to improve their performance on the new task, emulating how humans learn and adapt to new challenges (e.g., learning to ride a motorcycle is less challenging for someone who already knows how to ride a bicycle). It is also essential to identify the most relevant task for knowledge transfer when dealing with multiple learned tasks. Irrelevant knowledge can be harmful when learning new tasks [17, 20], resulting in flawed conclusions (e.g., misclassifying dolphins as fish instead of mammals could lead to misconceptions about their reproduction).

In this paper, we propose a *Discriminator-based Mode Affinity Score* (dMAS) to evaluate the similarity between generative tasks and present a new few-shot continual learning approach for the conditional generative adversarial network (cGAN) [21]. Our approach allows for seamless and efficient integration of new tasks’ knowledge by identifying and utilizing suitable information from previously learned modes. Here, each mode is corresponding to a generative task. Our framework

first evaluates the similarity between the existing modes and the new task using dMAS. It enables the identification of the most relevant modes whose knowledge can be leveraged for quick learning of the target task while preserving the knowledge of the existing modes. To this end, we add an additional mode to the generative model to represent the target task. This mode is assigned a class label derived from the labels of the relevant modes and the computed distances. Moreover, we incorporate memory replay [22, 23] to prevent catastrophic forgetting.

Extensive experiments are conducted on the MNIST [24], CIFAR-10 [25], and CIFAR-100 [25] datasets to validate the efficacy of our proposed approach. We empirically demonstrate the stability and robustness of dMAS, showing that it is invariant to the model initialization. Next, we apply the proposed measure to the continual learning scenario. Here, dMAS helps significantly reduce the number of the required data samples, and effectively utilize knowledge from the learned modes to learn new tasks. We achieve competitive results compared with baselines and the state-of-the-art approaches, including individual learning [21], sequential fine-tuning [4], multi-task learning [20], EWC-GAN [8], Lifelong-GAN [6], and CAM-GAN [5]. The contributions of our paper are summarized below:

- We propose a new discriminator-based mode-affinity measure (dMAS), to quantify the similarity between modes in conditional generative adversarial networks.
- We provide theoretical analysis (i.e., Theorem 1, Theorem 2) and empirical evaluation to demonstrate the robustness and stability of dMAS.
- We apply dMAS to transfer learning to reduce the required training data samples by leveraging the knowledge of the relevant learned modes to learn the new task.
- We present a new few-shot continual learning framework using dMAS for cGAN that expands the model by adding the target mode using the weighted label from the relevant learned modes.

2 Related Works

Continual or lifelong learning involves the problem of learning a new task while avoiding catastrophic forgetting [26, 27, 28]. This problem has been extensively studied in image classification problems [26, 29, 30, 31, 32, 33, 34, 35]. In image generation, previous works have addressed continual learning for a small number of tasks or modes in GANs [21]. These approaches, such as memory replay [33], have been proposed to prevent catastrophic forgetting [6, 36, 37]. However, as the number of modes increases, network expansion [38, 39, 40, 41, 42, 43] becomes necessary to efficiently learn new modes while retaining previously learned ones. Nevertheless, the excessive increase in the number of parameters remains a major concern.

The concept of task similarity has been widely investigated in transfer learning, which assumes that similar tasks share some common knowledge that can be transferred from one to another. However, existing approaches in transfer learning [26, 44, 45, 46, 47, 48, 49, 50, 51, 52] mostly focus on sharing the model weights from the learned tasks to the new task without explicitly identifying the closest tasks. In recent years, several works [17, 51, 53, 54, 55, 56, 57, 58, 59, 60, 61] have investigated the relationship between image classification tasks and applied relevant knowledge to improve overall performance. However, for the image generation tasks, the common approaches to quantify the similarity between tasks or modes are using common image evaluation metrics, such as Fréchet Inception Distance (FID) [62] and Inception Score (IS) [63]. While these metrics can provide meaningful similarity measures between two distributions of images, they do not capture the state of the generator and therefore may not be suitable for identifying relevant learned modes. For example, a model trained to generate images for one task may not be useful for another task, even if the images for both tasks are visually similar.

In continual learning for image generation [4, 5, 6, 8], mode-affinity has not been explicitly considered. Although some prior works [6, 8] have explored fine-tuning cGAN models (e.g., WGAN [64], BicycleGAN [65]) with regularization techniques, such as Elastic Weight Consolidation (EWC) [26], or the Knowledge Distillation [66], they did not focus on measuring mode similarity or selecting the closest modes for knowledge transfer. Other approaches use different assumptions such as global parameters for all modes and individual parameters for particular modes [5]. Their task distances also require a well-trained target generator, which is not suitable for few-shot continual learning.

3 Mode Affinity Score

We consider a conditional generative adversarial network (cGAN) that is trained on a set S of source generative tasks, where each task represents a distinct class of data. The cGAN consists of two key components: the generator \mathcal{G} and the discriminator \mathcal{D} . Each source generative task $a \in S$, which is characterized by data X_a and its labels y_a , corresponds to a specific *mode* in the well-trained generator \mathcal{G} . Let X_b denote the incoming target data.

Here, we propose a new mode-affinity measure, called Discriminator-based Mode Affinity Score (dMAS), to showcase the complexity involved in transferring knowledge between different modes in cGAN. This measure involves computing the expectation of Hessian matrices computed from the discriminator’s loss function. To calculate the dMAS, we begin by feeding the source data X_a into the discriminator \mathcal{D} to compute the corresponding loss. By taking the second-order derivative of the discriminator’s loss with respect to the input, we obtain the source Hessian matrix. Similarly, we repeat this process using the target data X_b as input to the discriminator, resulting in the target Hessian matrix. These matrices offer valuable insights into the significance of the model’s parameters concerning the desired data distribution. The dMAS is defined as the Fréchet distance between these Hessian matrices.

Definition 1 (Discriminator-based Mode Affinity Score). *Consider a well-trained cGAN with discriminator \mathcal{D} and the generator \mathcal{G} that has S learned modes. For the source mode $a \in S$, let X_a denote the real data, and \tilde{X}_a be the generated data from mode a of the generator \mathcal{G} . Given X_b is the target real data, H_a, H_b denote the expectation of the Hessian matrices derived from the loss function of the discriminator \mathcal{D} using $\{X_a, \tilde{X}_a\}$ and $\{X_b, \tilde{X}_a\}$, respectively. The distance from the source mode a to the target b is defined to be:*

$$s[a, b] := \frac{1}{\sqrt{2}} \text{trace} \left(H_a + H_b - 2H_a^{1/2} H_b^{1/2} \right)^{1/2}. \quad (1)$$

To simplify Equation (1), we approximate the Hessian matrices with their normalized diagonals as computing the full Hessian matrices in the large parameter space of neural networks can be computationally expensive. Hence, dMAS can be expressed as follows:

$$s[a, b] = \frac{1}{\sqrt{2}} \left\| H_a^{1/2} - H_b^{1/2} \right\|_F \quad (2)$$

Our proposed measure ranges from 0 to 1, with 0 indicating a perfect match and 1 indicating complete dissimilarity. Unlike the IS [63] and FID [62], dMAS is not limited to image data samples and can be applied to other types of data (e.g., text, multi-modal datasets). The proposed distance is asymmetric, reflecting the fact that knowledge transfer from a complex mode to a simpler one is easier than vice versa. The procedure to compute dMAS is outlined in function `dMAS()` in Algorithm 1.

4 Proposed Methods

4.1 Mode-Aware Transfer Learning

We apply the proposed mode-affinity score to transfer learning in an image generation scenario. The proposed similarity measure enables the identification of the closest modes or data classes to support the learning of the target mode. Here, we introduce a *mode-aware transfer learning* framework that quickly adapts a pre-trained cGAN model to learn the target mode. Particularly, we select the closest source mode from the pool of multiple learned modes based on the computed dMAS.

To leverage the knowledge of the closest mode for training the target mode, we assign the target data samples with labels of the closest mode. Subsequently, we use these modified target data samples to fine-tune the generator and discriminator of the pre-trained cGAN model. Figure 1(3A) illustrates the transfer learning method, where the data class 1 (i.e., cat images) is the most similar to the target data (i.e., leopard image) based on the computed dMAS. Hence, we assign the label of class 1 to the leopard images. The pre-trained GAN model uses this modified target data to quickly adapt the cat image generation to the leopard image generation. The pseudo-code is provided in Algorithm 2 in the appendix. By assigning the closest mode’s label to the target data samples, our method can effectively fine-tune the relevant parts of cGAN for learning the target mode. This approach helps improve the training process and reduces the number of required target training data samples.

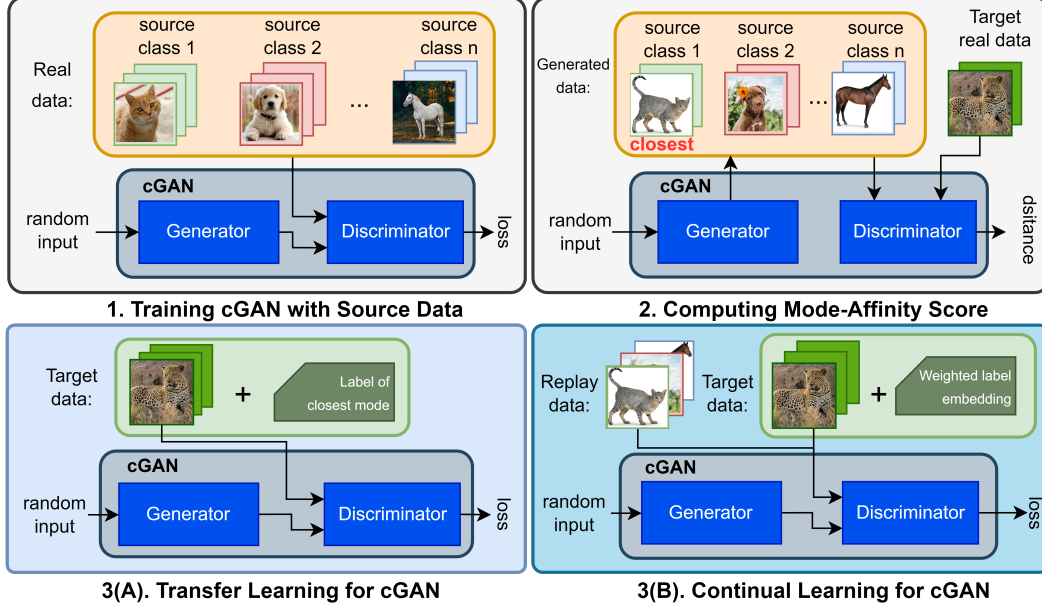


Figure 1: The overview of mode-aware transfer learning and continual learning frameworks for the conditional Generative Adversarial Network: **(1)** Representing source data classes using cGAN, **(2)** Computing the mode-affinity from each source mode to the target, **(3)** Fine-tuning the generative model using the target data and **(A)** the label of the closest mode for transfer learning, or **(B)** the weighted label embedding from relevant modes for continual learning.

4.2 Mode-Aware Continual Learning

We utilize the discriminator-based mode affinity score to few-shot continual learning for image generation. The goal is to train a lifelong learning cGAN model to learn new modes while avoiding catastrophic forgetting of existing modes. Consider a scenario where each generative task represents a distinct class of data. At time t , the cGAN model has S modes corresponding to S learned tasks. Here, we introduce a *mode-aware continual learning* framework that allows the model to add a new mode while retaining knowledge from previous modes.

We begin by embedding the numeric label of each data sample in the cGAN model, using an embedding layer in both the generator \mathcal{G} and the discriminator \mathcal{D} models. We then modify the cGAN model to enable it to take a linear combination of label embeddings for the target data. These label embeddings correspond to the most relevant modes, and the weights for these embedding features are associated with the computed dMAS from the related modes to the target. This enables the cGAN model to add a new target mode while maintaining all existing modes. Let $\text{emb}()$ denote the embedding layers in the generator \mathcal{G} and the discriminator \mathcal{D} , and C be the set of the relevant modes, $C = \{i_1^*, i_2^*, \dots, i_n^*\}$. The computed mode-affinity scores from these modes to the target are denoted as s_i^* . Let $\sum s_i^*$ denote the total distance from all the relevant modes to the target. The label embedding for the target data samples is described as follows:

$$\text{emb}(y_{\text{target}}) = \frac{s_{i_1^*}^*}{\sum s_i^*} \text{emb}(y_{\text{train}_{i_1^*}}) + \frac{s_{i_2^*}^*}{\sum s_i^*} \text{emb}(y_{\text{train}_{i_2^*}}) + \dots + \frac{s_{i_n^*}^*}{\sum s_i^*} \text{emb}(y_{\text{train}_{i_n^*}}) \quad (3)$$

In order to add the new target mode without forgetting the existing learned modes, we use the target data with the above label embedding to fine-tune the lifelong learning cGAN model. Additionally, we utilize memory replay [22, 23] to prevent catastrophic forgetting. Particularly, samples generated from relevant existing modes are used to fine-tune the cGAN model. Figure 1(3B) provides the overview of the proposed continual learning approach. During each iteration, training with the target data and replaying relevant existing modes are jointly implemented using an alternative optimization process. The pseudo-code of the continual learning framework is illustrated in Algorithm 1. Here, by applying the labels of the closest modes to the target data samples in the embedding space, the cGAN model can precisely update part of its model without sacrificing the generation performance of other

Algorithm 1: Mode-Aware Continual Learning for Conditional Generative Adversarial Networks

Data: Source data: (X_{train}, y_{train}) , Target data: X_{target}

Input: The generator \mathcal{G} and discriminator \mathcal{D} of cGAN

Output: Continual learning generator $\mathcal{G}_{\bar{\theta}}$ and discriminator $\mathcal{D}_{\bar{\theta}}$

Function dMAS ($X_a, y_a, X_b, \mathcal{G}, \mathcal{D}$):

Generate data \tilde{X}_a of class label y_a using the generator \mathcal{G}
Compute H_a from the loss of discriminator \mathcal{D} using $\{X_a, \tilde{X}_a\}$
Fine-tune $(\mathcal{G}, \mathcal{D})$ using X_b with y_a
Compute H_b from the loss of discriminator \mathcal{D} using $\{X_b, \tilde{X}_a\}$
return $s[a, b] = \frac{1}{\sqrt{2}} \|H_a^{1/2} - H_b^{1/2}\|_F$

Function Main:

Train $(\mathcal{G}_\theta, \mathcal{D}_\theta)$ with X_{train}, y_{train} ▷ Pre-train cGAN model
Construct S source modes, each from a data class in y_{train}
for $i = 1, 2, \dots, S$ **do**
 $s_i = \text{dMAS}(X_{train_i}, y_{train_i}, X_{target}, \mathcal{G}_\theta, \mathcal{D}_\theta)$ ▷ Find the closest modes
return closest mode(s): $i^* = \underset{i}{\operatorname{argmin}} s_i$
Generate data X_{i^*} of label i^* from closest mode(s) ▷ Fine-tune for continual learning
Define the target label embedding as a linear combination of the label embeddings of the closest modes, where the weights corresponding to s_{i^*} as follows:
$$\text{emb}(y_{target}) = \frac{s_{i_1^*}}{\sum s_i^*} \text{emb}(y_{train_{i_1^*}}) + \dots + \frac{s_{i_n^*}}{\sum s_i^*} \text{emb}(y_{train_{i_n^*}})$$

while θ not converged **do**
 Update $\mathcal{G}_\theta, \mathcal{D}_\theta$ using real data X_{target} and label embedding $\text{emb}(y_{target})$
 Replay $\mathcal{G}_\theta, \mathcal{D}_\theta$ with generated data X_{i^*} and label embedding $\text{emb}(y_{train_{i^*}})$
return $\mathcal{G}_{\bar{\theta}}, \mathcal{D}_{\bar{\theta}}$

existing modes. Overall, utilizing knowledge from past experience helps enhance the performance of cGAN in learning new modes while reducing the amount of the required training data samples.

Next, we provide a theoretical analysis of the proposed method. In Theorem 1, the introduction of a new mode through mode injection inherently involves a trade-off between the mode-adding ability and the potential performance loss compared to the original model. In essence, when incorporating a new mode, the performance of existing modes cannot be improved. The detailed proof of Theorem 1 is provided in Appendix B.

Theorem 1. Let X_a be the source data, characterized by the density function p_a . Let X_b be the data for the target mode with data density function p_b . Let θ denote the model's parameters. Consider the loss functions $L_a(\theta) = \mathbb{E}[l(X_a; \theta)]$ and $L_b(\theta) = \mathbb{E}[l(X_b; \theta)]$. Assume that both $L_a(\theta)$ and $L_b(\theta)$ are strictly convex and possess distinct global minima. Let X_n denote the mixture data of X_a and X_b described by $p_n = \alpha p_a + (1 - \alpha)p_b$, where $\alpha \in (0, 1)$. The corresponding loss function is given by $L_n(\theta) = \mathbb{E}[l(X_n; \theta)]$. Under these assumptions, it follows that $\theta^* = \arg \min_{\theta} L_n(\theta)$ satisfies:

$$L_a(\theta^*) > \min_{\theta} L_a(\theta) \quad (4)$$

5 Experimental Study

Our experiments aim to evaluate the effectiveness of the proposed mode-affinity measure in transfer learning and continual learning frameworks, as well as the consistency of the Discriminator-based Mode Affinity Score for cGAN. We consider a scenario where each generative task corresponds to a single data class in the MNIST [24], CIFAR-10 [25], and CIFAR-100 [25] datasets. Here, we compare the proposed frameworks with baselines and state-of-the-art approaches, including individual learning [21], sequential fine-tuning [4], multi-task learning [20], EWC-GAN [8], Lifelong-GAN [6], and CAM-GAN [5]. The results show the efficacy of our approach in terms of generative performance and the ability to learn new modes while preserving knowledge of the existing modes.

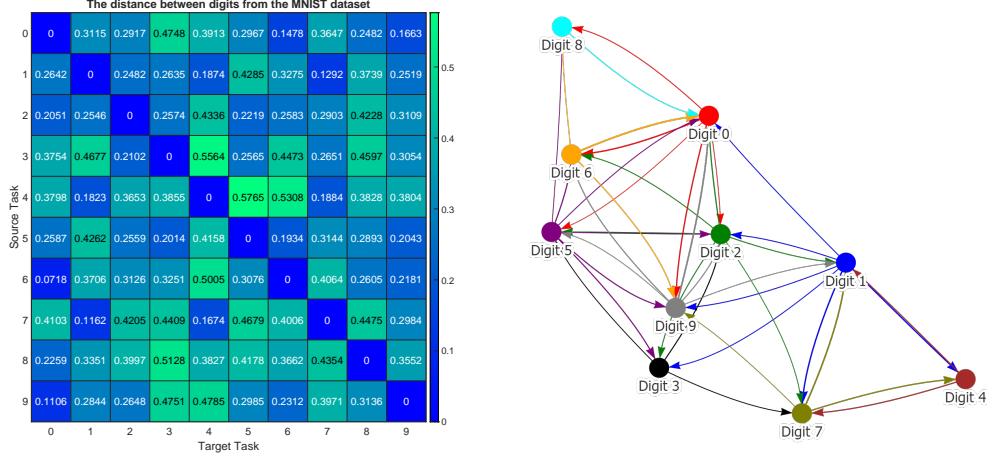


Figure 2: The average mode-affinity scores (left) between data classes (i.e., digits 0, 1, ..., 9) of the MNIST dataset in the cGAN model. The atlas plot (right) indicates the relationship between digits according to locations in space. The set $\{1, 4, 7\}$ and $\{0, 6, 8\}$ exhibit close connections. The remaining digits display a dense interconnection and a strong affiliation with other sets.

5.1 Generative Task Affinity Consistency

In the first experiment, the ten generative tasks are defined based on the MNIST dataset, where each task corresponded to generating a specific digit (i.e., 0, 1, ..., 9). For instance, task 0 aimed at generating images representing digit 0, while task 1 aimed at generating images depicting digit 1. The cGAN model was trained to generate images from the nine source tasks while considering one task as the target task. The cGAN model has nine modes corresponding to nine source tasks. The well-trained generator of this cGAN model served as the representation network for the source data. To evaluate the consistency of the closest modes for each target, we conduct 10 trial runs, in which the source cGAN model is initialized randomly. The mean and standard deviation of the mode-affinity scores between each pair of source-target modes are shown in Figure 2 and Figure 5, respectively. In the mean table from Figure 2, the columns denote the distance from each source mode to the given target. For instance, the first column indicates that digits 6 and 9 are closely related to the target digit 0. Similarly, the second column shows that digits 4 and 7 are the closest tasks to the incoming digit 1. The standard deviation table from Figure 5 indicates that the calculated distance is stable, as there are no overlapping fluctuations and the orders of similarity between tasks are preserved across 10 runs. In other words, this suggests that the tendency of the closest modes for each target remains consistent regardless of the initialization of cGAN. Thus, the computed mode-affinity score demonstrates consistent results. Additionally, we provide the atlas plot in Figure 2 which gives an overview of the relationship between the digits based on the computed distances. The plot reveals that digits 1, 4, 7 exhibit a notable similarity, while digits 0, 6, 8 are closely related. This plot provides a useful visualization to showcase the pattern and similarity among different digits.

Analogously, we define ten generative tasks for the CIFAR-10 dataset, each corresponding to a specific object, such as airplane, automobile, bird, cat, deer, dog, frog, horse, ship, and truck. Following the previous experiment, one task is designated as the target task, while the others are the source tasks used to train the cGAN model for image generation. The generator of the well-trained cGAN model serves as the representation network for the source tasks. We present the mean and standard deviation of computed mode-affinity scores between each pair of source-target modes over 10 trial runs in Figure 3 and Figure 6, respectively. The mean table in Figure 3 shows the average distance of each source mode from the target (e.g., trucks are similar to automobiles, and cats are closely related to dogs). The standard deviation table in Figure 6 demonstrates the stability of the results across different initialization of cGAN. The consistent findings suggest that the computed distances from the CIFAR-10 dataset are reliable. Furthermore, in Figure 3, we include the atlas plot which presents an overview of the relationship between the objects based on the computed mode-affinity scores. The plot reveals that automobile, truck, ship, and airplane have a strong connection, while the other classes (i.e., bird, cat, dog, deer, horse, frog) also exhibit a significant resemblance.

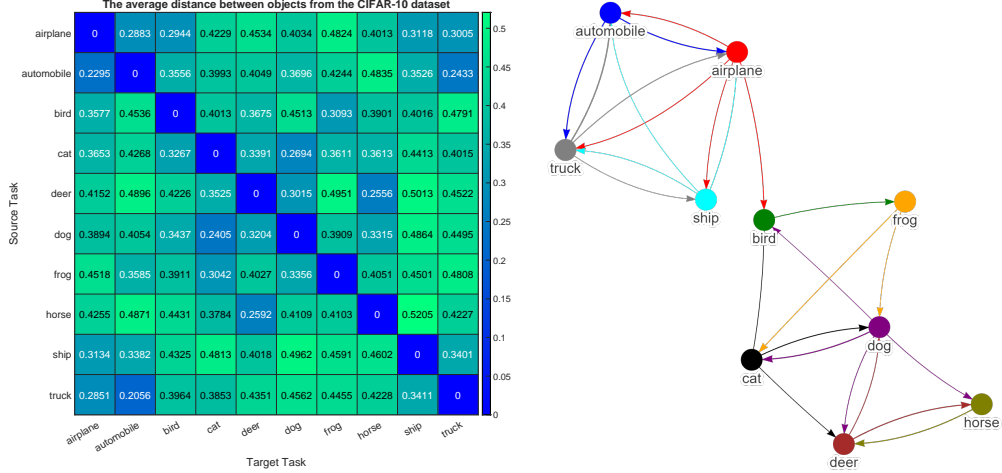


Figure 3: The average mode-affinity scores (left) between data classes (e.g., airplane, automobile, bird) of the CIFAR-10 dataset using the conditional generative adversarial networks. The atlas plot (right) indicates the relationship between CIFAR-10 objects according to locations in space.

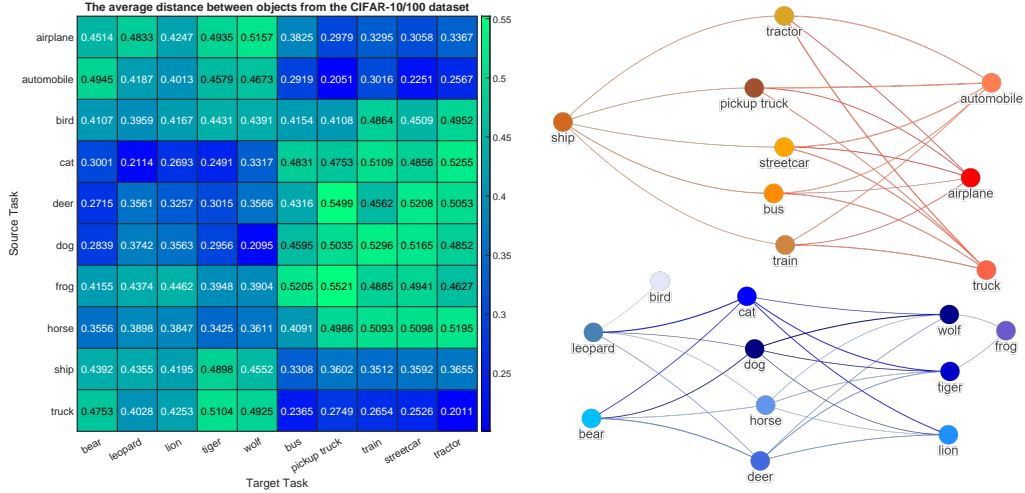


Figure 4: The average mode-affinity scores (left) between data classes of the CIFAR-10 and CIFAR-100 datasets using the conditional generative adversarial networks. The atlas plot (right) indicates the relationship between CIFAR-10 and CIFAR-100 objects according to locations in space.

Next, the CIFAR-100 dataset is utilized to define ten target tasks, each corresponding to a specific image class, such as bear, leopard, lion, tiger, wolf, bus, pickup truck, train, streetcar, and tractor. For this experiment, the cGAN model is trained on the entire CIFAR-10 dataset to generate images from ten classes or modes. Figure 4 and Figure 7 respectively display the mean and standard deviation of the computed mode-affinity scores between the source-target modes. The mean table in Figure 4 indicates the average distance from each CIFAR-10 source mode to the CIFAR-100 target mode. Notably, the target tasks of generating bear, leopard, lion, tiger, and wolf images are closely related to the group of cat, deer, and dog. Specifically, cat images are closely related to leopard, lion, and tiger images. Moreover, the target modes of generating bus, pickup truck, streetcar, and tractor images are highly related to the group of automobile, truck, airplane, and ship. The standard deviation table in Figure 7 also indicates that the computed distances are consistent across different trial runs, demonstrating the stability of the computed mode-affinity scores. Thus, the distances computed between the CIFAR-100 modes and the CIFAR-10 modes are reliable and consistent. In addition, Figure 4 includes an atlas plot that provides a visual representation of the relationships between objects based on the computed distances. The plot reveals a strong connection between the vehicles, such as tractors, trucks, and trains, as well as a notable closeness between the animal classes, such

Table 1: Comparison of the mode-aware transfer learning framework (MA-Transfer Learning) for conditional generative adversarial networks against other approaches in terms of FID scores.

MNIST				
APPROACH	TARGET	10-SHOT	20-SHOT	100-SHOT
INDIVIDUAL LEARNING [21]	DIGIT 0	34.25	27.17	19.62
SEQUENTIAL FINE-TUNING [6]	DIGIT 0	29.68	24.22	16.14
MULTI-TASK LEARNING [20]	DIGIT 0	26.51	20.74	10.95
MA-TRANSFER LEARNING	DIGIT 0	12.64	7.51	5.53
CIFAR-10				
APPROACH	TARGET	10-SHOT	20-SHOT	100-SHOT
INDIVIDUAL LEARNING [21]	TRUCK	89.35	81.74	72.18
SEQUENTIAL FINE-TUNING [6]	TRUCK	76.93	70.39	61.41
MULTI-TASK LEARNING [20]	TRUCK	72.06	65.38	55.29
MA-TRANSFER LEARNING	TRUCK	51.05	44.93	36.74
CIFAR-100				
APPROACH	TARGET	10-SHOT	20-SHOT	100-SHOT
INDIVIDUAL LEARNING [21]	LION	87.91	80.21	72.58
SEQUENTIAL FINE-TUNING [6]	LION	77.56	70.76	61.33
MULTI-TASK LEARNING [20]	LION	71.25	67.84	56.12
MA-TRANSFER LEARNING	LION	51.08	46.97	37.51

as lions, tigers, cats, and dogs. This plot serves as a useful tool for visualizing the similarity and relationship between different objects in the CIFAR-10 and CIFAR-100 datasets and can help to identify relevant data classes for the target class.

5.2 Transfer Learning Performance

Our transfer learning framework utilizes the computed mode-affinity scores between generative tasks in the MNIST [24], CIFAR-10 [25], and CIFAR-100 [25] datasets for learning the target tasks. Specifically, we use this distance metric to identify the closest mode to the target mode and then fine-tune cGAN accordingly. To this end, we assign the target data samples with the labels of the closest mode and use these newly-labeled samples to train the cGAN model. By doing so, the generative model can benefit from the knowledge learned from the closest mode for quick adaptation in learning the target mode. We compare our method with three baselines: individual learning [21], sequential learning [6], and multi-task learning [20]. Next, we demonstrate the performance comparison of our proposed mode-aware transfer learning approach with other approaches for the target tasks with 10-shot, 20-shot, and 100-shot in MNIST, CIFAR-10, and CIFAR-100 datasets (i.e., the target dataset only has 10, 20, 100 data samples). Particularly, for the MNIST dataset, we consider generating digits 0 and 1 as the target modes. As shown in Table 1 and Table 3, our method outperforms individual learning, sequential fine-tuning, and multi-task learning approaches significantly. Since the individual learning model lacks training data, it can only produce low-quality samples. On the other hand, the sequential fine-tuning and multi-task learning models use the entire source dataset while training the target mode, which results in better performance than the individual learning method. However, they cannot identify the most relevant source mode and data, thus, making them inefficient compared with our proposed mode-aware transfer learning approach. In other words, the proposed approach can generate high-quality images with fewer target training samples. Notably, the proposed approach can achieve better results using only 20% of data samples. For more complex tasks, such as generating cat and truck images in CIFAR-10 and lion and bus images in CIFAR-100, our approach achieves competitive results to other methods while requiring only 10% training samples. Hence, the mode-aware transfer learning framework using the Discriminator-based Mode Affinity Score can effectively identify relevant source modes and utilize their knowledge for learning the target mode.

5.3 Continual Learning Performance

We apply the computed mode-affinity scores between generative tasks in the MNIST [24], CIFAR-10 [25], and CIFAR-100 [25] datasets to the mode-aware continual learning framework. Particularly,

Table 2: Comparison of the mode-aware continual learning framework (MA-Continual Learning) for conditional generative adversarial networks against other approaches in terms of FID scores.

MNIST				
APPROACH	TARGET	\mathcal{P}_{target}	$\mathcal{P}_{closest}$	$\mathcal{P}_{average}$
SEQUENTIAL FINE-TUNING [6]	DIGIT 0	16.14	26.51	25.94
MULTI-TASK LEARNING [20]	DIGIT 0	10.95	5.48	6.01
EWC-GAN [8]	DIGIT 0	8.91	7.27	7.83
LIFELONG-GAN [6]	DIGIT 0	8.27	6.64	7.07
CAM-GAN [5]	DIGIT 0	6.86	6.18	6.03
MA-CONTINUAL LEARNING	DIGIT 0	6.15	5.88	5.57
CIFAR-10				
APPROACH	TARGET	\mathcal{P}_{target}	$\mathcal{P}_{closest}$	$\mathcal{P}_{average}$
SEQUENTIAL FINE-TUNING [6]	TRUCK	61.41	65.11	64.48
MULTI-TASK LEARNING [20]	TRUCK	55.29	33.61	35.51
EWC-GAN [8]	TRUCK	44.65	35.39	35.18
LIFELONG-GAN [6]	TRUCK	41.94	35.18	34.83
CAM-GAN [5]	TRUCK	37.28	34.57	34.01
MA-CONTINUAL LEARNING	TRUCK	35.78	34.85	33.91
CIFAR-100				
APPROACH	TARGET	\mathcal{P}_{target}	$\mathcal{P}_{closest}$	$\mathcal{P}_{average}$
SEQUENTIAL FINE-TUNING [6]	LION	63.75	66.31	65.57
MULTI-TASK LEARNING [20]	LION	56.12	35.79	37.28
EWC-GAN [8]	LION	46.92	38.59	36.55
LIFELONG-GAN [6]	LION	43.95	38.01	36.71
CAM-GAN [5]	LION	40.49	37.43	36.67
MA-CONTINUAL LEARNING	LION	38.62	36.48	35.89

we select the top-2 closest mode to the target and leverage their knowledge for quick adaptation in learning the target task while preventing catastrophic forgetting. First, we construct a label embedding for the target data samples based on the label embeddings of the top-2 closest modes and the computed distances, as shown in Equation (3). Next, we fine-tune the source cGAN model with the newly-labeled target samples, while also implementing memory replay to avoid catastrophic forgetting of the existing modes. We compare our framework with sequential fine-tuning [6], multi-task learning [20], EWC-GAN [8], lifelong-GAN [6], and CAM-GAN [5] for the few-shot generative task with 100 target data samples. We report the FID scores of the images from the target mode, top-2 closest modes, and the average of all modes in Table 2 and Table 4. By selectively choosing and utilizing the relevant knowledge from learned modes, our approach significantly outperforms the conventional training methods (i.e., sequential fine-tuning, and multi-task learning) for generative tasks, such as generating digit 0, truck, lion, digit 1, cat, and bus images. The results further demonstrate that our proposed mode-aware continual learning approach outperforms EWC-GAN [8] in all tasks in MNIST, CIFAR-10, and CIFAR-100 datasets. Moreover, our model also achieves highly competitive results in comparison to lifelong-GAN [6] and CAM-GAN [5], showcasing its outstanding performance on the target task. Although we observed a slight degradation in the performance of the top-2 closest modes due to the trade-off discussed in Theorem 1, our lifelong learning model demonstrates better overall performance when considering all the learned modes.

6 Conclusion

We introduce a new method to measure the similarity between generative tasks in conditional generative adversarial networks. Our distance, called the Discriminator-based Mode Affinity Score, is based on the expectation of the Hessian matrices derived from the discriminator’s loss function. This measure provides insight into the difficulty of extracting useful knowledge from existing modes to learn new tasks. We apply this mode-affinity measure to transfer learning and few-shot continual learning, leveraging relevant learned modes for quick adaptation to new target modes. Our experiments demonstrate the effectiveness of our methods compared to conventional fine-tuning methods and other state-of-the-art continual learning approaches.

References

- [1] OpenAI, “Gpt-3.5.” Computer software, 2021.
- [2] A. Vaswani, N. Shazeer, N. Parmar, J. Uszkoreit, L. Jones, A. N. Gomez, L. Kaiser, and I. Polosukhin, “DALL•E: Creating images from text.” OpenAI, 2021.
- [3] M. Westerlund, “The emergence of deepfake technology: A review,” *Technology innovation management review*, vol. 9, no. 11, 2019.
- [4] Y. Wang, C. Wu, L. Herranz, J. Van de Weijer, A. Gonzalez-Garcia, and B. Raducanu, “Transferring gans: generating images from limited data,” in *Proceedings of the European Conference on Computer Vision (ECCV)*, pp. 218–234, 2018.
- [5] S. Varshney, V. K. Verma, P. Srijith, L. Carin, and P. Rai, “Cam-gan: Continual adaptation modules for generative adversarial networks,” *Advances in Neural Information Processing Systems*, vol. 34, pp. 15175–15187, 2021.
- [6] M. Zhai, L. Chen, F. Tung, J. He, M. Nawhal, and G. Mori, “Lifelong gan: Continual learning for conditional image generation,” in *Proceedings of the IEEE/CVF international conference on computer vision*, pp. 2759–2768, 2019.
- [7] C. P. Le, Y. Zhou, J. Ding, and V. Tarokh, “Supervised encoding for discrete representation learning,” in *ICASSP 2020-2020 IEEE International Conference on Acoustics, Speech and Signal Processing (ICASSP)*, pp. 3447–3451, IEEE, 2020.
- [8] A. Seff, A. Beatson, D. Suo, and H. Liu, “Continual learning in generative adversarial nets,” *arXiv preprint arXiv:1705.08395*, 2017.
- [9] A. Vaswani, N. Shazeer, N. Parmar, J. Uszkoreit, L. Jones, A. N. Gomez, L. Kaiser, and I. Polosukhin, “Attention is all you need,” *Advances in neural information processing systems*, vol. 30, 2017.
- [10] J. Devlin, M.-W. Chang, K. Lee, and K. Toutanova, “Bert: Pre-training of deep bidirectional transformers for language understanding,” *arXiv preprint arXiv:1810.04805*, 2018.
- [11] J. Howard and S. Ruder, “Universal language model fine-tuning for text classification,” in *Proceedings of the 56th Annual Meeting of the Association for Computational Linguistics (Volume 1: Long Papers)*, pp. 328–339, 2018.
- [12] C. P. Le, L. Dai, M. Johnston, Y. Liu, M. Walker, and R. Ghanadan, “Improving open-domain dialogue evaluation with a causal inference model,” *Diversity in Dialogue Systems: 13th International Workshop on Spoken Dialogue System Technology (IWSDS)*, 2023.
- [13] T. Brown, B. Mann, N. Ryder, M. Subbiah, J. D. Kaplan, P. Dhariwal, A. Neelakantan, P. Shyam, G. Sastry, A. Askell, *et al.*, “Language models are few-shot learners,” *Advances in neural information processing systems*, vol. 33, pp. 1877–1901, 2020.
- [14] N. Elaraby, S. Barakat, and A. Rezk, “A conditional gan-based approach for enhancing transfer learning performance in few-shot hcr tasks,” *Scientific Reports*, vol. 12, no. 1, p. 16271, 2022.
- [15] Y. Guo, H. Shi, A. Kumar, K. Grauman, T. Rosing, and R. Feris, “Spottune: transfer learning through adaptive fine-tuning,” in *Proceedings of the IEEE/CVF conference on computer vision and pattern recognition*, pp. 4805–4814, 2019.
- [16] W. Ge and Y. Yu, “Borrowing treasures from the wealthy: Deep transfer learning through selective joint fine-tuning,” in *Proceedings of the IEEE conference on computer vision and pattern recognition*, pp. 1086–1095, 2017.
- [17] C. P. Le, J. Dong, M. Soltani, and V. Tarokh, “Task affinity with maximum bipartite matching in few-shot learning,” in *International Conference on Learning Representations*, 2022.
- [18] Y. Cui, Y. Song, C. Sun, A. Howard, and S. Belongie, “Large scale fine-grained categorization and domain-specific transfer learning,” in *Proceedings of the IEEE conference on computer vision and pattern recognition*, pp. 4109–4118, 2018.
- [19] S. Azizi, B. Mustafa, F. Ryan, Z. Beaver, J. Freyberg, J. Deaton, A. Loh, A. Karthikesalingam, S. Kornblith, T. Chen, *et al.*, “Big self-supervised models advance medical image classification,” in *Proceedings of the IEEE/CVF International Conference on Computer Vision*, pp. 3478–3488, 2021.

- [20] T. Standley, A. Zamir, D. Chen, L. Guibas, J. Malik, and S. Savarese, “Which tasks should be learned together in multi-task learning?,” in *International Conference on Machine Learning*, pp. 9120–9132, PMLR, 2020.
- [21] M. Mirza and S. Osindero, “Conditional generative adversarial nets,” *arXiv preprint arXiv:1411.1784*, 2014.
- [22] A. Robins, “Catastrophic forgetting, rehearsal and pseudorehearsal,” *Connection Science*, vol. 7, no. 2, pp. 123–146, 1995.
- [23] W. Chenshen, L. HERRANZ, L. Xialei, *et al.*, “Memory replay gans: Learning to generate images from new categories without forgetting [c],” in *The 32nd International Conference on Neural Information Processing Systems, Montréal, Canada*, pp. 5966–5976, 2018.
- [24] Y. LeCun, C. Cortes, and C. Burges, “Mnist handwritten digit database,” *AT&T Labs [Online]*. Available: <http://yann.lecun.com/exdb/mnist>, vol. 2, p. 18, 2010.
- [25] A. Krizhevsky, G. Hinton, *et al.*, “Learning multiple layers of features from tiny images,” *CiteSeer*, 2009.
- [26] J. Kirkpatrick, R. Pascanu, N. Rabinowitz, J. Veness, G. Desjardins, A. A. Rusu, K. Milan, J. Quan, T. Ramalho, A. Grabska-Barwinska, *et al.*, “Overcoming catastrophic forgetting in neural networks,” *Proceedings of the national academy of sciences*, vol. 114, no. 13, pp. 3521–3526, 2017.
- [27] M. McCloskey and N. J. Cohen, “Catastrophic interference in connectionist networks: The sequential learning problem,” in *Psychology of learning and motivation*, vol. 24, pp. 109–165, Elsevier, 1989.
- [28] G. A. Carpenter and S. Grossberg, “A massively parallel architecture for a self-organizing neural pattern recognition machine,” *Computer vision, graphics, and image processing*, vol. 37, no. 1, pp. 54–115, 1987.
- [29] A. Achille, G. B. Mbeng, and S. Soatto, “The dynamic distance between learning tasks: From kolmogorov complexity to transfer learning via quantum physics and the information bottleneck of the weights of deep networks,” *NeurIPS Workshop on Integration of Deep Learning Theories*, 2018.
- [30] S.-A. Rebuffi, A. Kolesnikov, G. Sperl, and C. H. Lampert, “icarl: Incremental classifier and representation learning,” in *Proceedings of the IEEE conference on Computer Vision and Pattern Recognition*, pp. 2001–2010, 2017.
- [31] V. K. Verma, K. J. Liang, N. Mehta, P. Rai, and L. Carin, “Efficient feature transformations for discriminative and generative continual learning,” in *Proceedings of the IEEE/CVF Conference on Computer Vision and Pattern Recognition*, pp. 13865–13875, 2021.
- [32] F. Zenke, B. Poole, and S. Ganguli, “Continual learning through synaptic intelligence,” in *International conference on machine learning*, pp. 3987–3995, PMLR, 2017.
- [33] C. Wu, L. Herranz, X. Liu, J. Van De Weijer, B. Raducanu, *et al.*, “Memory replay gans: Learning to generate new categories without forgetting,” *Advances in Neural Information Processing Systems*, vol. 31, 2018.
- [34] P. Singh, V. K. Verma, P. Mazumder, L. Carin, and P. Rai, “Calibrating cnns for lifelong learning,” *Advances in Neural Information Processing Systems*, vol. 33, pp. 15579–15590, 2020.
- [35] J. Rajasegaran, S. Khan, M. Hayat, F. S. Khan, and M. Shah, “itaml: An incremental task-agnostic meta-learning approach,” in *Proceedings of the IEEE/CVF Conference on Computer Vision and Pattern Recognition*, pp. 13588–13597, 2020.
- [36] Y. Cong, M. Zhao, J. Li, S. Wang, and L. Carin, “Gan memory with no forgetting,” *Advances in Neural Information Processing Systems*, vol. 33, pp. 16481–16494, 2020.
- [37] A. Rios and L. Itti, “Closed-loop memory gan for continual learning,” *arXiv preprint arXiv:1811.01146*, 2018.
- [38] J. Yoon, E. Yang, J. Lee, and S. J. Hwang, “Lifelong learning with dynamically expandable networks,” *arXiv preprint arXiv:1708.01547*, 2017.
- [39] J. Xu and Z. Zhu, “Reinforced continual learning,” *Advances in Neural Information Processing Systems*, vol. 31, 2018.

- [40] M. Zhai, L. Chen, J. He, M. Nawhal, F. Tung, and G. Mori, “Piggyback gan: Efficient lifelong learning for image conditioned generation,” in *Computer Vision—ECCV 2020: 16th European Conference, Glasgow, UK, August 23–28, 2020, Proceedings, Part XXI* 16, pp. 397–413, Springer, 2020.
- [41] A. Mallya and S. Lazebnik, “Packnet: Adding multiple tasks to a single network by iterative pruning,” in *Proceedings of the IEEE conference on Computer Vision and Pattern Recognition*, pp. 7765–7773, 2018.
- [42] M. Masana, T. Tuytelaars, and J. van de Weijer, “Ternary feature masks: continual learning without any forgetting,” *arXiv preprint arXiv:2001.08714*, vol. 4, no. 5, p. 6, 2020.
- [43] J. Rajasegaran, M. Hayat, S. H. Khan, F. S. Khan, and L. Shao, “Random path selection for continual learning,” *Advances in Neural Information Processing Systems*, vol. 32, 2019.
- [44] D. L. Silver and K. P. Bennett, “Guest editor’s introduction: special issue on inductive transfer learning,” *Machine Learning*, vol. 73, no. 3, pp. 215–220, 2008.
- [45] C. Finn, X. Y. Tan, Y. Duan, T. Darrell, S. Levine, and P. Abbeel, “Deep spatial autoencoders for visuomotor learning,” in *Robotics and Automation (ICRA), 2016 IEEE International Conference on*, pp. 512–519, IEEE, 2016.
- [46] L. Mihalkova, T. Huynh, and R. J. Mooney, “Mapping and revising markov logic networks for transfer learning,” in *AAAI*, vol. 7, pp. 608–614, 2007.
- [47] A. Niculescu-Mizil and R. Caruana, “Inductive transfer for bayesian network structure learning,” in *Artificial Intelligence and Statistics*, pp. 339–346, 2007.
- [48] Z. Luo, Y. Zou, J. Hoffman, and L. F. Fei-Fei, “Label efficient learning of transferable representations across domains and tasks,” in *Advances in Neural Information Processing Systems*, pp. 164–176, 2017.
- [49] A. S. Razavian, H. Azizpour, J. Sullivan, and S. Carlsson, “Cnn features off-the-shelf: An astounding baseline for recognition,” in *Proceedings of the 2014 IEEE Conference on Computer Vision and Pattern Recognition Workshops, CVPRW ’14*, (Washington, DC, USA), pp. 512–519, IEEE Computer Society, 2014.
- [50] S. J. Pan and Q. Yang, “A survey on transfer learning,” *IEEE Transactions on Knowledge and Data Engineering*, vol. 22, pp. 1345–1359, Oct 2010.
- [51] A. R. Zamir, A. Sax, W. B. Shen, L. Guibas, J. Malik, and S. Savarese, “Taskonomy: Disentangling task transfer learning,” in *2018 IEEE Conference on Computer Vision and Pattern Recognition (CVPR)*, IEEE, 2018.
- [52] S. Chen, C. Zhang, and M. Dong, “Coupled end-to-end transfer learning with generalized fisher information,” in *Proceedings of the IEEE Conference on Computer Vision and Pattern Recognition*, pp. 4329–4338, 2018.
- [53] C. P. Le, M. Soltani, R. Ravier, and V. Tarokh, “Task-aware neural architecture search,” in *ICASSP 2021-2021 IEEE International Conference on Acoustics, Speech and Signal Processing (ICASSP)*, pp. 4090–4094, IEEE, 2021.
- [54] C. P. Le, M. Soltani, J. Dong, and V. Tarokh, “Fisher task distance and its application in neural architecture search,” *IEEE Access*, vol. 10, pp. 47235–47249, 2022.
- [55] C. P. Le, M. Soltani, R. Ravier, and V. Tarokh, “Improved automated machine learning from transfer learning,” *arXiv e-prints*, pp. arXiv–2103, 2021.
- [56] A. Aloui, J. Dong, C. P. Le, and V. Tarokh, “Causal knowledge transfer from task affinity,” *arXiv preprint arXiv:2210.00380*, 2022.
- [57] A. Pal and V. N. Balasubramanian, “Zero-shot task transfer,” 2019.
- [58] K. Dwivedi and G. Roig., “Representation similarity analysis for efficient task taxonomy and transfer learning,” in *CVPR*, IEEE Computer Society, 2019.
- [59] A. Achille, M. Lam, R. Tewari, A. Ravichandran, S. Maji, C. Fowlkes, S. Soatto, and P. Perona, “Task2Vec: Task Embedding for Meta-Learning,” *arXiv e-prints*, p. arXiv:1902.03545, Feb. 2019.
- [60] A. Y. Wang, L. Wehbe, and M. J. Tarr, “Neural taskonomy: Inferring the similarity of task-derived representations from brain activity,” *BioRxiv*, p. 708016, 2019.

- [61] T. Standley, A. Zamir, D. Chen, L. Guibas, J. Malik, and S. Savarese, “Which tasks should be learned together in multi-task learning?,” in *Proceedings of the 37th International Conference on Machine Learning* (H. D. III and A. Singh, eds.), vol. 119 of *Proceedings of Machine Learning Research*, pp. 9120–9132, PMLR, 13–18 Jul 2020.
- [62] M. Heusel, H. Ramsauer, T. Unterthiner, B. Nessler, and S. Hochreiter, “Gans trained by a two time-scale update rule converge to a local nash equilibrium,” *Advances in neural information processing systems*, vol. 30, 2017.
- [63] T. Salimans, I. Goodfellow, W. Zaremba, V. Cheung, A. Radford, and X. Chen, “Improved techniques for training gans,” *Advances in neural information processing systems*, vol. 29, 2016.
- [64] M. Arjovsky, S. Chintala, and L. Bottou, “Wasserstein generative adversarial networks,” in *International conference on machine learning*, pp. 214–223, PMLR, 2017.
- [65] J.-Y. Zhu, R. Zhang, D. Pathak, T. Darrell, A. A. Efros, O. Wang, and E. Shechtman, “Toward multimodal image-to-image translation,” *Advances in neural information processing systems*, vol. 30, 2017.
- [66] G. Hinton, O. Vinyals, and J. Dean, “Distilling the knowledge in a neural network,” *arXiv preprint arXiv:1503.02531*, 2015.
- [67] I. Gulrajani, F. Ahmed, M. Arjovsky, V. Dumoulin, and A. C. Courville, “Improved training of wasserstein gans,” *Advances in neural information processing systems*, vol. 30, 2017.
- [68] K. Yonekura, N. Miyamoto, and K. Suzuki, “Inverse airfoil design method for generating varieties of smooth airfoils using conditional wgan-gp,” *arXiv preprint arXiv:2110.00212*, 2021.

A Experimental Setup

In this work, we construct 30 generative tasks based on popular datasets such as MNIST [24], CIFAR-10 [25], and CIFAR-100 [25]. For MNIST, we define ten distinct generative tasks, each focused on generating a specific digit (i.e., 0, 1, ..., 9). Task 0, for example, is designed to generate the digit 0, while task 1 generates the digit 1, and so on. For the CIFAR-10 dataset, we also construct ten generative tasks, with each task aimed at generating a specific object category such as airplane, automobile, bird, cat, deer, dog, frog, horse, ship, and truck. Similarly, for the CIFAR-100 dataset, we create ten target tasks, each corresponding to a specific image class, including bear, leopard, lion, tiger, wolf, bus, pickup truck, train, streetcar, and tractor.

To represent the generative tasks, we utilize the conditional Wasserstein GAN with Gradient Penalty (cWGAN-GP) model [67, 68]. In each experiment, we select a specific task as the target task, while considering the other tasks as source tasks. To represent these source tasks, we train the cWGAN-GP model on their respective datasets. This enables us to generate high-quality samples that are representative of the source tasks. Once trained, we can use the cWGAN-GP model as the representation network for the generative tasks. This model is then applied to our proposed task-aware transfer learning and continual learning frameworks. We compare our method against several approaches, including individual learning [21], sequential fine-tuning [4], multi-task learning [20], EWC-GAN [8], Lifelong-GAN [6], and CAM-GAN [5]. Individual learning [21] involves training the cGAN model on a specific task in isolation. In sequential fine-tuning [4], the cGAN model is trained sequentially on source and target tasks. Multi-task learning [20], on the other hand, involves training a cGAN model on a joint dataset created from both the source and target tasks. Our method is designed to improve on these approaches by enabling the continual learning of generative tasks while mitigating catastrophic forgetting.

B Theoretical Analysis

We first recall the definition of the GAN’s discriminator loss as follows:

Definition 2 (Discriminator Loss). *Let $x = \{x_1, \dots, x_m\}$ be the real data samples, z denote the random vector, and θ_D be the discriminator’s parameters. \mathcal{D} is trained to maximize the probability of assigning the correct label to both training real samples and generated samples $\mathcal{G}(z)$ from the generator \mathcal{G} . The objective of the discriminator is to maximize the following function:*

$$\nabla_{\theta_D} \sum_{i=1}^m \left[\log \mathcal{D}(x^{(i)}) + \log \left(1 - \mathcal{D}(\mathcal{G}(z^{(i)})) \right) \right] \quad (5)$$

We recall the definition of Fisher Information matrix (FIM) [54] as follows:

Definition 3 (Fisher Information). *Given dataset X , let N denote a neural network with weights θ , and the negative log-likelihood loss function $L(\theta) := L(\theta, X)$. FIM is described as follows:*

$$F(\theta) = \mathbb{E} \left[\nabla_{\theta} L(\theta) \nabla_{\theta} L(\theta)^T \right] = -\mathbb{E} \left[H(L(\theta)) \right] \quad (6)$$

Next, we present the proof of Theorem 1 and proof of Theorem 2.

Theorem 1. *Let X_a be the source data, characterized by the density function p_a . Let X_b be the data for the target mode with data density function p_b . Let θ denote the model’s parameters. Consider the loss functions $L_a(\theta) = \mathbb{E}[l(X_a; \theta)]$ and $L_b(\theta) = \mathbb{E}[l(X_b; \theta)]$. Assume that both $L_a(\theta)$ and $L_b(\theta)$ are strictly convex and possess distinct global minima. Let X_n denote the mixture data of X_a and X_b described by $p_n = \alpha p_a + (1 - \alpha) p_b$, where $\alpha \in (0, 1)$. The corresponding loss function is given by $L_n(\theta) = \mathbb{E}[l(X_n; \theta)]$. Under these assumptions, it follows that $\theta^* = \arg \min_{\theta} L_n(\theta)$ satisfies:*

$$L_a(\theta^*) > \min_{\theta} L_a(\theta) \quad (7)$$

Proof of Theorem 1. We have:

$$L_a(\theta^*) \geq \min_{\theta} L_a(\theta)$$

Assuming that $L_a(\theta^*) = \min_{\theta} L_a(\theta)$. By the tower property, we have that

$$L_b(\theta) = \alpha L_a(\theta) + (1 - \alpha) L_n(\theta)$$

Thus, $\nabla L_b(\theta^*) = 0$ and $\nabla L_a(\theta^*) = 0$. Hence,

$$\nabla L_n(\theta^*) = 0$$

By strict convexity, L_n and L_a have the same global minimums, which contradicts our assumptions. By way of contradiction, we conclude the result. \square

Next, we present Theorem 2, which establishes a fundamental connection between the computations of the Fisher Information matrix (FIM) and the expectation of the Hessian matrix from the discriminator loss. Our proposed distance is closely linked to FIM derived from cGAN's loss function with an optimal discriminator. This means that our distance metric remains consistent, regardless of the current state of the discriminator.

Theorem 2 (Relationship between dMAS and Fisher Information). *Let X_a, X_b denote the source and target data. Given a source cGAN (i.e., the generator \mathcal{G} and the discriminator \mathcal{D}), let p_r, p_g denote the real and generated data distributions over sample $x_a \in X_a$, respectively. Assume that the optimal set of parameters for \mathcal{D}_a exists for cGAN's loss function. Let $H_{\theta_{\mathcal{D}}}$ denote the Hessian matrix obtained from \mathcal{D} . This matrix is closely related to FIM and the second-order derivative of cGAN's loss function in which \mathcal{D} is assumed to be optimal.*

$$H_{\theta_{\mathcal{D}}} = \nabla_{\theta_{\mathcal{D}}}^2 L(\mathcal{G}, \mathcal{D}^*) \quad (8)$$

Proof of Theorem 2. The loss function of the GAN model with respect to the discriminator and its parameters θ can be described as follows:

$$L(\mathcal{D}_a) = \mathbb{E}_{X_a}[\log \mathcal{D}(X_a)] + \mathbb{E}_{X_b}[\log(1 - \mathcal{D}(X_b))] \quad (9)$$

Consider the case where the discriminator aims to identify the generated data samples of task a with label $y = 0$ and the real data samples of task b with label $y = 1$. In other words, $\mathcal{D}(X_a)$ can be described as $p_{\theta}(Y = 0|X_a)$. Similarly, $(1 - \mathcal{D}(X_b))$ can be described as $p_{\theta}(Y = 1|X_b)$. Hence, the loss function of the discriminator \mathcal{D}_a is simplified as follows:

$$L(\mathcal{D}_a) = \mathbb{E}_{X_a}[\log p_{\theta}(Y = 0|X_a)] + \mathbb{E}_{X_b}[\log p_{\theta}(Y = 1|X_b)] \quad (10)$$

Let p_a, p_b denote the true distribution of the data from task a, b , respectively. The data distribution is described as follows:

$$p_{\theta}(x) = p_{\theta}(y = 0|x)p_a(x) + p_{\theta}(y = 1|x)p_b(x) \quad (11)$$

The Hessian matrix $H_{a,a}$ for task a is computed using the discriminator with the data x_a (i.e., $X \sim X_a$). Assume that the discriminator is very good and can identify correctly all data samples. In other words, $p_{\theta}(y = 1|x) = 0$. The second derivative of the discriminator's loss function for task a is described as follows:

$$\begin{aligned} \nabla_{\theta}^2 L_a(\mathcal{D}_a) &= \mathbb{E}_{X \sim X_a}[\nabla_{\theta}^2 \log p_{\theta}(x)] \\ &= \mathbb{E}_{X \sim X_a}[\nabla_{\theta}^2 \log p_{\theta}(y = 0|x)] + \mathbb{E}_{X \sim X_a}[\nabla_{\theta}^2 \log p_a(x)] \\ &= \mathbb{E}_{X \sim X_a}[\nabla_{\theta}^2 \log p_{\theta}(y = 0|x)] + 0 \\ &= F_{a,a} \end{aligned} \quad (12)$$

Similarly, the Hessian matrix $F_{a,b}$ for task b is computed using the discriminator with the data x_b (i.e., $X \sim X_b$). Here, $p_{\theta}(y = 0|x) = 0$. The second derivative of the discriminator's loss function for task b is described as follows:

$$\begin{aligned} \nabla_{\theta}^2 L_b(\mathcal{D}_a) &= \mathbb{E}_{X \sim X_b}[\nabla_{\theta}^2 \log p_{\theta}(x)] \\ &= \mathbb{E}_{X \sim X_b}[\nabla_{\theta}^2 \log p_{\theta}(y = 1|x)] + \mathbb{E}_{X \sim X_b}[\nabla_{\theta}^2 \log p_b(x)] \\ &= \mathbb{E}_{X \sim X_b}[\nabla_{\theta}^2 \log p_{\theta}(y = 1|x)] + 0 \\ &= F_{a,b} \end{aligned} \quad (13)$$

Thus, the Discriminator-based Mode Affinity Score $s[a, b]$ can be described as follows:

$$s[a, b] = \frac{1}{\sqrt{2}} \left\| \nabla_{\theta}^2 L_a(\mathcal{D}_a)^{1/2} - \nabla_{\theta}^2 L_b(\mathcal{D}_a)^{1/2} \right\|_F = \frac{1}{\sqrt{2}} \left\| F_{a,a}^{1/2} - F_{a,b}^{1/2} \right\|_F \quad (14)$$

\square

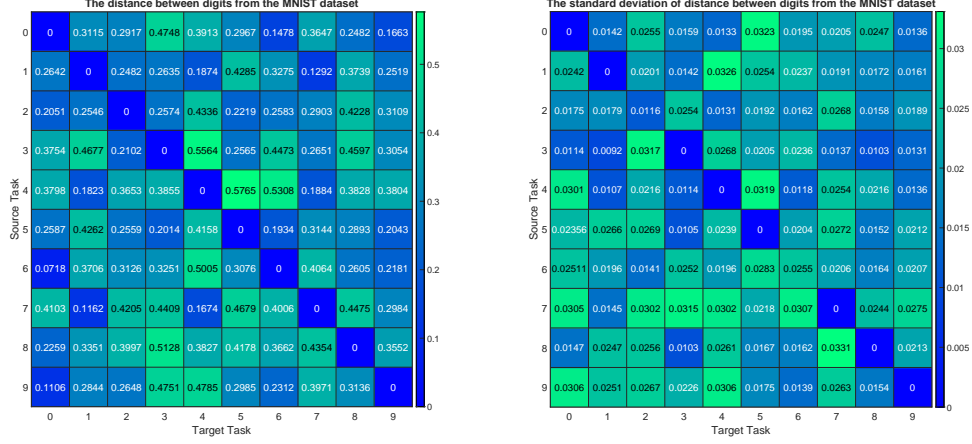


Figure 5: The mean (left) and standard deviation (right) of computed mode-affinity scores between data classes (i.e., digits 0, 1, . . . , 9) of the MNIST dataset using the conditional generative adversarial networks.

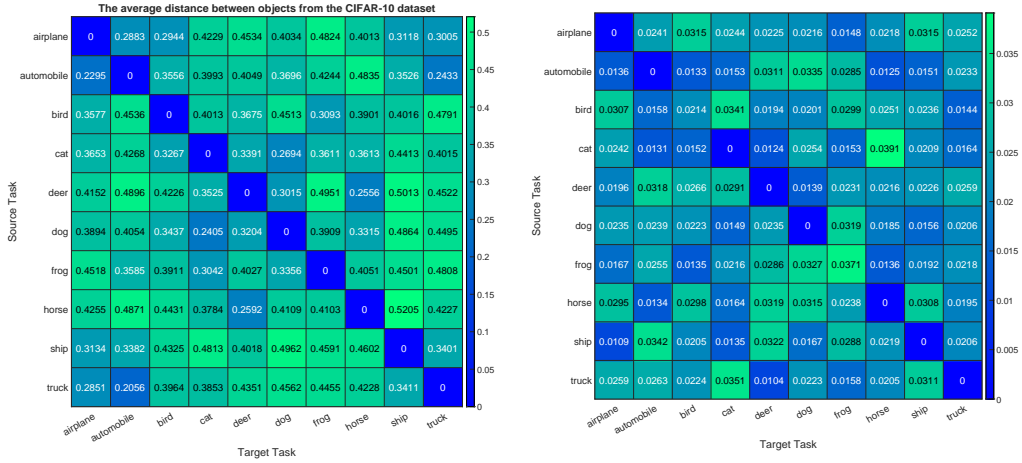


Figure 6: The mean (left) and standard deviation (right) of computed mode-affinity scores between data classes (i.e., airplane, automobile, bird,..., truck) of the CIFAR-10 dataset using the conditional generative adversarial networks.

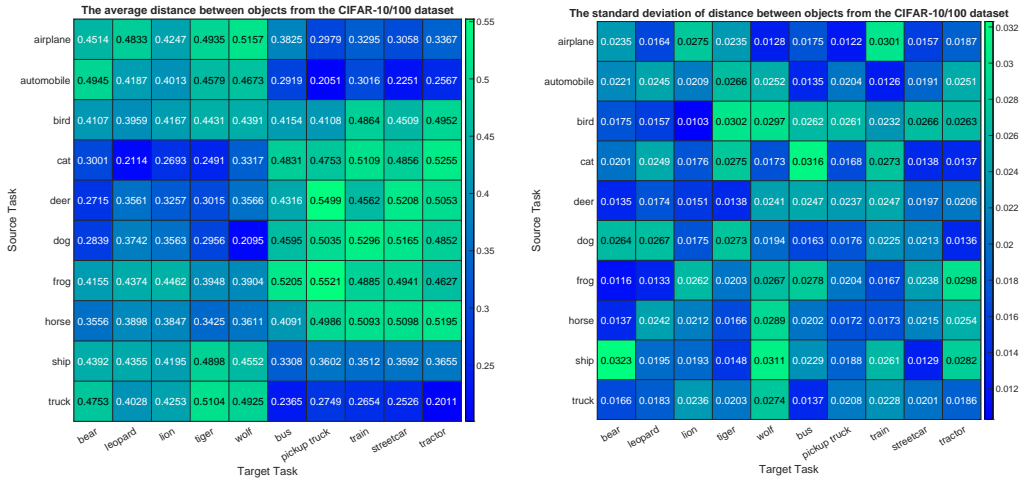


Figure 7: The mean (left) and standard deviation (right) of computed mode-affinity scores between data classes of the CIFAR-10 and CIFAR-100 datasets using the conditional generative adversarial networks.

Table 3: Comparison of generation performance in terms of FID scores between the mode-aware transfer learning framework (MA-Transfer Learning) for conditional generative adversarial networks against other approaches for the tasks of generating digit 1, cat, and bus images.

MNIST				
APPROACH	TARGET	10-SHOT	20-SHOT	100-SHOT
INDIVIDUAL LEARNING [21]	DIGIT 1	35.07	29.62	20.83
SEQUENTIAL FINE-TUNING [6]	DIGIT 1	28.35	24.79	15.85
MULTI-TASK LEARNING [20]	DIGIT 1	26.98	21.56	10.68
MA-TRANSFER LEARNING	DIGIT 1	11.35	7.12	5.28
CIFAR-10				
APPROACH	TARGET	10-SHOT	20-SHOT	100-SHOT
INDIVIDUAL LEARNING [21]	CAT	80.25	74.46	65.18
SEQUENTIAL FINE-TUNING [6]	CAT	73.51	68.23	59.08
MULTI-TASK LEARNING [20]	CAT	68.73	61.32	50.65
MA-TRANSFER LEARNING	CAT	47.39	40.75	32.46
CIFAR-100				
APPROACH	TARGET	10-SHOT	20-SHOT	100-SHOT
INDIVIDUAL LEARNING [21]	BUS	94.82	89.01	78.47
SEQUENTIAL FINE-TUNING [6]	BUS	88.03	79.51	67.33
MULTI-TASK LEARNING [20]	BUS	80.06	76.33	61.59
MA-TRANSFER LEARNING	BUS	57.16	50.06	41.81

Table 4: Comparison of generation performance in terms of FID scores between the mode-aware continual learning framework (MA-Continual Learning) for conditional generative adversarial networks against other approaches for the tasks of generating digit 1, cat, and bus images.

MNIST				
APPROACH	TARGET	\mathcal{P}_{target}	$\mathcal{P}_{closest}$	$\mathcal{P}_{average}$
SEQUENTIAL FINE-TUNING [6]	DIGIT 1	15.85	25.43	25.01
MULTI-TASK LEARNING [20]	DIGIT 1	10.68	5.41	5.93
EWC-GAN [8]	DIGIT 1	9.12	8.52	7.98
LIFELONG-GAN [6]	DIGIT 1	8.28	7.15	7.05
CAM-GAN [5]	DIGIT 1	6.67	6.35	6.11
MA-CONTINUAL LEARNING	DIGIT 1	5.93	5.74	5.52
CIFAR-10				
APPROACH	TARGET	\mathcal{P}_{target}	$\mathcal{P}_{closest}$	$\mathcal{P}_{average}$
SEQUENTIAL FINE-TUNING [6]	CAT	59.08	62.94	62.14
MULTI-TASK LEARNING [20]	CAT	50.65	33.25	35.01
EWC-GAN [8]	CAT	42.67	36.31	35.19
LIFELONG-GAN [6]	CAT	39.83	35.83	34.85
CAM-GAN [5]	CAT	36.79	35.07	34.21
MA-CONTINUAL LEARNING	CAT	35.18	34.55	33.68
CIFAR-100				
APPROACH	TARGET	\mathcal{P}_{target}	$\mathcal{P}_{closest}$	$\mathcal{P}_{average}$
SEQUENTIAL FINE-TUNING [6]	BUS	67.33	70.52	68.84
MULTI-TASK LEARNING [20]	BUS	61.59	36.84	37.98
EWC-GAN [8]	BUS	49.78	39.61	37.59
LIFELONG-GAN [6]	BUS	43.51	39.15	37.44
CAM-GAN [5]	BUS	42.64	38.82	37.21
MA-CONTINUAL LEARNING	BUS	41.29	38.05	36.62

Algorithm 2: Mode-Aware Transfer Learning for Conditional Generative Adversarial Networks

Data: Source data: (X_{train}, y_{train}) , Target data: X_{target}

Input: The generator \mathcal{G} and discriminator \mathcal{D} of cGAN

Output: Target generator $\mathcal{G}_{\bar{\theta}}$

Function dMAS ($X_a, y_a, X_b, \mathcal{G}, \mathcal{D}$) :

Generate data \tilde{X}_a of class label y_a using the generator \mathcal{G}
 Compute H_a from the loss of discriminator \mathcal{D} using $\{X_a, \tilde{X}_a\}$
 Fine-tune $(\mathcal{G}, \mathcal{D})$ using X_b with y_a
 Compute H_b from the loss of discriminator \mathcal{D} using $\{X_b, \tilde{X}_a\}$
return $s[a, b] = \frac{1}{\sqrt{2}} \|H_a^{1/2} - H_b^{1/2}\|_F$

Function Main:

Train $(\mathcal{G}_{\theta}, \mathcal{D}_{\theta})$ with X_{train}, y_{train} ▷ Pre-train cGAN model
 Construct S source modes, each from a data class in y_{train}
for $i = 1, 2, \dots, S$ **do**
 | $s_i = \text{dMAS}(X_{train_i}, y_{train_i}, X_{target}, \mathcal{G}_{\theta}, \mathcal{D}_{\theta})$ ▷ Find the closest modes
return closest mode(s): $i^* = \underset{i}{\operatorname{argmin}} s_i$
▷ Fine-tune with the target task
while θ not converged **do**
 | Update $\mathcal{G}_{\theta}, \mathcal{D}_{\theta}$ using real data X_{target} and closest source label $y_{train_{i^*}}$
return $\mathcal{G}_{\bar{\theta}}$
